Determination of Component Volumes of Lipid Bilayers from Simulations

Horia I. Petrache,* Scott E. Feller,§ and John F. Nagle*#
*Department of Physics and #Department of Biological Sciences, Carnegie Mellon University, Pittsburgh, Pennsylvania 15213, and §Department of Chemistry, Whitman College, Walla Walla, Washington 99362 USA

ABSTRACT An efficient method for extracting volumetric data from simulations is developed. The method is illustrated using a recent atomic-level molecular dynamics simulation of L_α phase 1,2-dipalmitoyl-*sn*-glycero-3-phosphocholine bilayer. Results from this simulation are obtained for the volumes of water (V_W), lipid (V_L), chain methylenes (V_2), chain terminal methyls (V_3), and lipid headgroups (V_H), including separate volumes for carboxyl (V_{COO}), glyceryl (V_{gl}), phosphoryl (V_{PO_4}), and choline (V_{chol}) groups. The method assumes only that each group has the same average volume regardless of its location in the bilayer, and this assumption is then tested with the current simulation. The volumes obtained agree well with the values V_W and V_L that have been obtained directly from experiment, as well as with the volumes V_H, V_2, and V_3 that require certain assumptions in addition to the experimental data. This method should help to support and refine some assumptions that are neccessary when interpreting experimental data.

INTRODUCTION

Computer simulations, such as molecular dynamics or Monte Carlo, can, in principle, provide a complete description of lipid bilayer structure. Because of finite computing resources, simulations are limited spatially and temporally. A typical simulation box contains only a 20-nm^2 patch of a single bilayer, many orders of magnitude smaller than the macroscopic dispersions studied by experiment. The longest simulations are on the order of nanoseconds, much shorter than the longest observed relaxation times (Dufourc et al., 1992). Both limitations may introduce artifacts, to which one may add uncertainties in the potential functions, although these are considerably reduced by comparing simulation results on simpler systems to experiment. It is nevertheless valuable to test simulation results on lipid bilayers with data on lipid bilayers wherever possible. A traditional test has used the deuterium order parameters obtained from NMR, and a more recent test compares electron density profiles with those obtained from x-ray scattering. However, it should be stressed that the flow of information between simulation and experiment should not be in only one direction. The simulations give much information that is not obtainable from experiment. This information can then be used to test assumptions common in the interpretation of experimental data; examples include the derivation of the area/molecule A, both from NMR (Nagle, 1993) and from x-ray scattering (Nagle et al., 1996).

The focus of this paper is on volumetric information, which is critical in discussing the energetics of lipid bilayers (Nagle, 1980). As with NMR and x-ray scattering, volumetric information provides tests of simulations against direct experimental results, notably the volume per lipid molecule (V_L) (Wiener et al., 1988; Nagle and Wilkinson, 1978), as well as the volume (V_W) of the water molecules in the bulk water region. It also allows comparison with experimental results that require interpretation (Nagle and Wiener, 1988), particularly the volume per methylene (V_2), the volume per methyl (V_3), and the volume of the headgroup (V_H). Furthermore, the simulations provide volumetric information about smaller molecular components, such as the choline, the phosphoryl group, the carboxyl groups, and the glyceryl group, that are even more difficult to obtain experimentally (Wiener and White, 1992).

The particular contribution of this paper is to provide a simple and efficient way to obtain volume information from simulations. This requires some explanation, because it might seem that volumetric information would flow automatically from a complete set of atomic coordinates. The straightforward procedure would be to define dividing surfaces between neighboring molecules. Building spheres around the geometric centers is unsatisfactory, because the construction will not fill the whole space. Something similar to Wigner-Seitz cells would be well defined and fill up all space, but either approach would be computationally demanding. In contrast, the method we propose requires only positional histograms for the various component groups; these histograms, which are accumulated during the course of a simulation, are part of the primary output and are used for a variety of other purposes, such as providing electron density profiles.

There is also a fundamental issue regarding the definition of the dividing surfaces. To illustrate the delicacy of defining such dividing surfaces, consider the very simple picture of a water molecule as a sphere, so that there is only one parameter, its molecular radius a_W. It is unlikely that there are any criteria that would determine a_W more accurately than at the 1% level. However, a 1% uncertainty in a_W (e.g., from 1.928 Å to 1.949 Å) means that one cannot discriminate between values of 30 Å^3 and 31 Å^3 in V_W, which is an

Received for publication 6 December 1996 and in final form 6 February 1997.

Address reprint requests to Dr. John F. Nagle, Department of Physics, Carnegie Mellon University, Pittsburgh, PA 15213. Tel.: 412-268-2764; Fax: 412-681-0648; E-mail: nagle@andrew.cmu.edu.

0006-3495/97/05/2237/06 $2.00

unacceptably large uncertainty in V_W. (One would require pressure differences of over 600 atmospheres to bring about this change in the average volume of pure water.) Even so, one could argue that the average $\langle V_W \rangle$ over the whole system is not affected, because shifting the dividing surface adds to one molecule what it takes from a neighbor. Therefore, the dividing surface is not crucial for a one-component system, but for a multicomponent system with intimate mixing of the components, arbitrary dividing surfaces lead to arbitrary and significantly different values for the different components. There is an obvious alternative procedure for a one-component solution, namely, dividing the total volume of the system by the number of molecules to obtain the molecular volume. It is this simple concept that we will develop in this paper to extract the volumes of the substituent groups, e.g., the headgroup or the methylene groups, of inhomogeneous systems such as lipid bilayers.

DEVELOPMENT OF THE METHOD

Definition of number density $n(z)$

A coordinate system is chosen such that the bilayer lies in the xy plane and z is the direction of the bilayer normal. The simulation box is divided into slices of thickness Δz, perpendicular to z, as shown in Fig. 1. In the simulation used in this paper, Δz was chosen to be 0.134 Å. The number of occurrences $N(z)$ of a particular molecular group in each slice is counted to obtain $N(z)$ in the form of a histogram. For good statistical averaging, such counts are made frequently during the time course of the simulation, and $N(z)$ is the accumulated number of counts (although checks should be made to avoid gross movements in the center of mass of the entire bilayer). The number density $n(z)$ is then defined as

$$n(z) = \frac{N(z)}{V_S}, \tag{1}$$

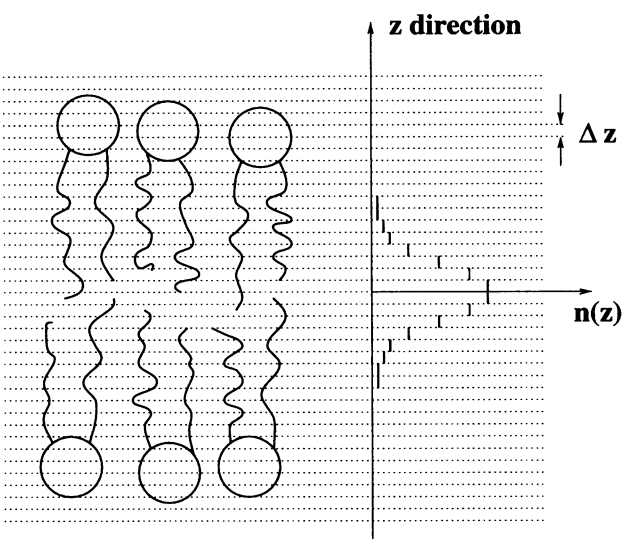

FIGURE 1 Schematic number density histogram for terminal methyls.

where V_S is the slice volume. An example of the terminal methyl groups on the hydrocarbon chains is shown in Fig. 1.

Within the framework of this general definition, there are still options regarding details of the counting procedure, namely, how does one decide whether a particular molecular group is in a particular slice? There are several possibilities:

1. Count the whole group if its center of mass is in the slice.
2. Count the whole group if the geometric center of its van der Waals volume is in the slice.
3. Count the whole group if its heaviest atom is in the slice.
4. Count only that fraction of the group that is in the slice. There are two possibilities within this option. The fractional part can be determined either on a mass basis (4a) or on the basis of the number of electrons (4b).

The differences between these distributions depend on the molecular shape and composition as well as on the binning size Δz. Although the examples to be shown in this paper employ method 4b, the following general development applies for all options.

Definition of component volume

Consider an example of a binary liquid mixture of molecular species A and B, for which the number densities are given by

$$n_A(z) = \frac{N_A(z)}{V_S} \quad \text{and} \quad n_B(z) = \frac{N_B(z)}{V_S}. \tag{2}$$

Letting V_A and V_B be the volumes of groups A and B, respectively, these component volumes will be required to ensure volume conservation,

$$V_A N_A(z) + V_B N_B(z) = V_S. \tag{3}$$

Notice that Eq. 3 allows no void space. Dividing by V_S, we have

$$V_A n_A(z) + V_B n_B(z) = 1. \tag{4}$$

Defining a probability $p_\xi(z) = V_\xi n_\xi(z)$, we may rewrite Eq. 4 as

$$p_A(z) + p_B(z) = 1, \tag{5}$$

which expresses the volume conservation in terms of probability conservation: at position z there is probability $p_A(z)$ of being within the volume of a molecule of type A and, correspondingly, probability $1 - p_A(z)$ of being within the volume of a molecule of type B. Therefore, our definitions do not focus on "free volume," although that concept may be included, as will be discussed later.

If the binary mixture is homogeneous, so that $n_A(z)$ and $n_B(z)$ are constants as a function of z, then the basic Eq. 4 does not suffice to define the component volumes V_A and V_B uniquely, because an increase in V_A can be accompanied by a decrease in V_B such that Eq. 4 is satisfied for each z slice. In contrast, if the number densities $n_A(z)$ and $n_B(z)$ are

different in two different z slices, then there is only one solution for V_A and V_B that works in both slices. Thus it is the inhomogeneity of composition in the z direction that allows Eq. 4 to provide a unique solution for the component volumes.

The preceding treatment relies on a crucial assumption, that the component volume of a group is independent of z. This assumption is inconsistent, for example, with the conventional expectation that methylene groups near the center of the bilayer have larger volumes than those near the headgroups because they are more "fluid." This assumption is not inconsistent, however, with the expectation that there is more free volume near the center of the bilayer, as will be discussed later. If this assumption is not true, then it is unlikely that Eq. 4 can be satisfied simultaneously at all z, because there are many more z values, all with different number densities, than there are component volumes. Therefore, the set of equations in Eq. 4 is overdetermined, and the breakdown of this assumption should appear as deviations of the left-hand side from unity as a function of z. We may note that the same assumption has been employed by Wiener and White (1992) and was tested by examining a quantity similar to the left-hand side of Eq. 4 as a function of z.

Basic procedure

To illustrate the basic procedure, let us consider a specific model of the lipid bilayer system as being a mixture of four components: terminal methyls on the hydrocarbon chains, each with volume V_3; methylenes on the hydrocarbon chains, each with volume V_2; headgroups, each with volume V_H, that include all of the lipid molecule except the chain methylenes and methyls; and water molecules, each with volume V_W. Generalizing Eq. 4 to four components, we wish to find V_3, V_2, V_H, and V_W such that the total probability

$$p_T(z) \equiv V_3 n_3(z) + V_2 n_2(z) + V_H n_H(z) + V_W n_W(z) \quad (6)$$

is ideally equal to 1 for all values of z. Given the number distributions from simulations, it is straightforward to find the four volumetric parameters, V_3, V_2, V_H, and V_W, by minimizing

$$F(V_3, V_2, V_H, V_W) = \sum_i (p_T(z_i) - 1)^2. \quad (7)$$

Of course, this procedure can be generalized to other models for the partitioning of the lipid.

Simulations

The example developed in this paper uses a recent 1,2-dipalmitoyl-*sn*-glycero-3-phosphocholine (DPPC) simulation of Feller et al. (manuscript in preparation). However, we emphasize that the above method is independent of any particular simulation. Briefly, these simulations were performed for a bilayer consisting of 72 lipids and 29.1 waters/lipid using the program CHARMM. The average area per lipid was fixed at 62.9 Å^2. The normal box dimension was allowed to vary with a normal pressure of 1 atmosphere. The simulation temperature was 50°C. The parameter set PARMM22b4b was employed with Ewald summation of the coulombic interactions. The basic time step was 2 fs, and the total time of the simulation was 1.1 ns. In our calculations we used symmetrized number density distributions $n(z)$ obtained from the electron distribution (method 4b). The distributions were averaged over 800 snapshots taken every picosecond after an equilibration time of 300 ps.

RESULTS

Fig. 2 shows our result for the quantity $p_T(z)$ defined in Eq. 6. The results for the volumes are given in the column labeled 4c in Table 1. Table 1 also shows the total lipid volume V_L obtained by adding the volumes of all the substituent groups.

The rms deviation from unity of the probablility in Fig. 2 is 2%, but this is not all attributable to the breakdown of the basic assumption of constancy of the component volumes. In particular, the large deviations of $p_T(z)$ from 1 in the headgroup region from 15 to 25 Å are due to the "halo" effect of the headgroups. This effect is easiest to explain if the headgroups are counted according to their geometric center (option 2 above, Development of the Method). Relative to the surrounding molecular groups, the headgroups have a large volume from which the other groups are

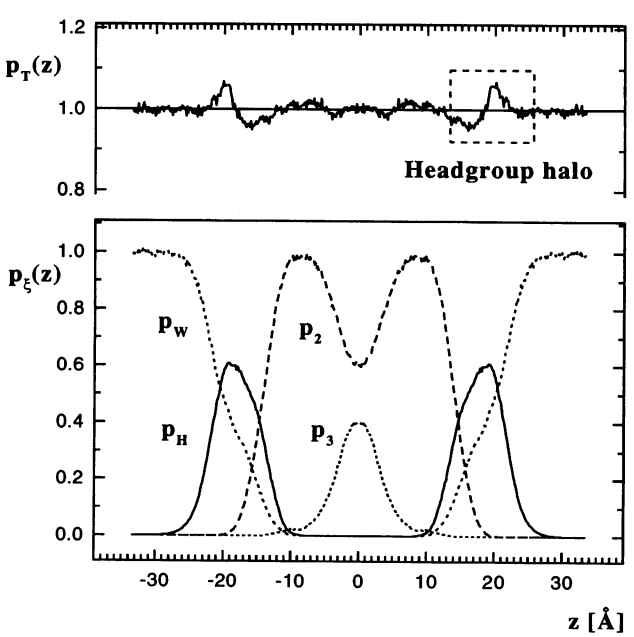

FIGURE 2 Four component (4c) model. (*Upper graph*) The total probability function $p_T(z)$ in Eq. 6. (*Lower graph*) The probability functions $p_\xi(z) = V_\xi n_\xi(z)$ obtained from simulations (Feller et al., manuscript in preparation) for the four molecular groups: CH_3 (p_3), CH_2 (p_2), headgroup (p_H), and water (p_W).

TABLE 1 Results for component volumes (in Å^3; $r = V_3/V_2$)

	4c	7c	Eq. 8	Eq. 9	Exp
V_L	1219	1218	1219	1217	1232*
V_W	30.3	30.4	30.4	30.4	30.3
V_3	52.6	53.6	—	—	54.6#
V_2	28.2	28.0	—	—	28.7#
r	1.87	1.92	—	—	1.9§
V_H	324	326	—	—	319¶
V_{COO}	—	41	—	—	—
V_{gl}	—	72	—	—	—
V_{PO_4}	—	59	—	—	—
V_{chol}	—	113	—	—	—

*Nagle and Wiener (1988).
#Depends weakly upon choice of r.
§r chosen from simulations.
¶Sun et al. (1994).

excluded. If the headgroup distribution is very sharp, then there would be a sharp peak in $p_T(z)$ surrounded by a "halo" consisting of a z interval with $p_T(z) = 0$, because this space is occupied by the headgroups. As the headgroup distribution broadens, the headgroup peak broadens, but a shallower halo remains. This halo effect is reduced further by use of electron counting, which spreads out the headgroup over its volume, but the high concentration of electrons on the phosphorous prevents this from being a uniform counting over the headgroup volume, so a halo effect is still expected, and is observed in Fig. 2.

One possibility for minimizing the halo effect is to add a smearing convolution function for the headgroup number density distribution. For the present data, in which $n_H(z)$ has been obtained from electron distribution, that smearing function must account for the inhomogeneity of the headgroup, making the treatment complicated and arbitrary. Our preferred way to minimize the halo effect is to divide the headgroup into smaller components. We will parse the headgroup in the same way as Wiener and White (1992). Compared to the preceding 4c model, which had a total of four components, the headgroup component will now be divided into four smaller components: the carboxyl groups, with volume V_{COO}; the glyceryl group, with volume V_{gl}; the phosphoryl group, with volume V_{PO_4}; and the choline group, with volume V_{chol}. This seven-component (7c) model should reduce the halo effect because the components are of more nearly equal size. The 7c model also gives additional information regarding the volumes of these molecular substituents of the headgroup.

The result for $p_T(z)$ for the 7c model is shown in Fig. 3. This result is visibly improved compared to Fig. 2, and the rms deviation is decreased to 1%. The results for the volumes are presented in the 7c column of Table 1.

ALTERNATIVE METHODS FOR OBTAINING V_L

There are two additional methods of calculating V_L from simulation results. The first uses the relation

$$V_L = AD/2 - N_W V_W, \tag{8}$$

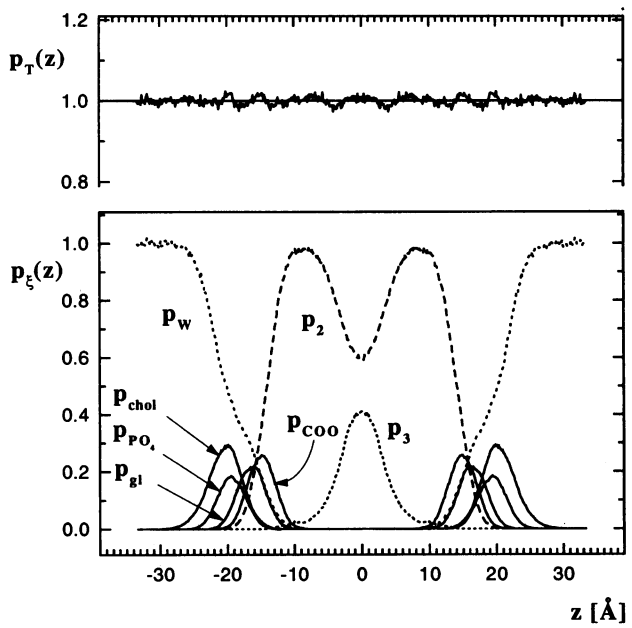

FIGURE 3 Seven component (7c) model. (*Upper graph*) The total probability function $p_T(z)$ in Eq. 6. (*Lower graph*) The probability functions $p_\xi(z) = V_\xi n_\xi(z)$ obtained from simulations (Feller et al., manuscript in preparation) for the molecular groups: CH_3 (p_3), CH_2 (p_2), carboxyl (p_{COO}), glyceryl (p_{gl}), phosphoryl (p_{PO_4}), choline (p_{chol}), and water (p_W).

where A is the area per lipid molecule, D is the height of the simulation box, and N_W is the number of waters per lipid. In the simulation (Feller et al., manuscript in preparation), D = 66.91 Å, N_W = 29.08, and A = 62.9 Å^2. We choose V_W = 30.4 Å^3 by examining $n_W(z)$ in the water region (see Fig. 4); this is the primary limit on the accuracy of the method. Then, using Eq. 8, we obtain V_L = 1219 Å^3.

The second way employs the "water deficit" integral (I_W), which is the integral between the bulk water density level and the actual water density profile (see Fig. 4). V_L can then be expressed as

$$V_L = (AI_W/2)V_W. \tag{9}$$

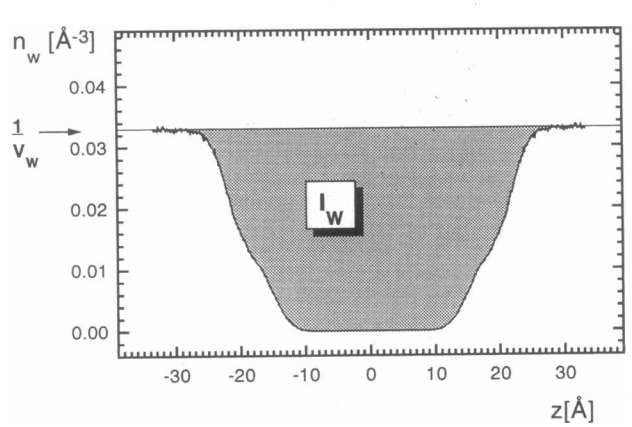

FIGURE 4 Water number density profile obtained from simulations (Feller et al., manuscript in preparation).

Using the simulated value of $A = 62.9$ Å^2 and $V_W = 30.4$ Å^3, Eq. 9 yields $V_L = 1217$ Å^3. The principal errors come from V_W and I_W.

DISCUSSION

We first discuss the results for V_L. The results of the various calculations (4c, 7c, Eq. 8, and Eq. 9) are compiled in Table 1, along with the experimental result obtained by Nagle and Wiener (1988). It may be noted that errors in the experimental values are 2 Å^3, as determined by the standard methods of analysis of the experiments, or by comparing results from different experiments, which give specific volumes v_m (in ml/g of fully hydrated DPPC at 45°C) of 1.005 (Blazyk et al., 1975), 1.003 (Nagle and Wilkinson, 1978), and 1.006 (Laggner et al., 1987; Wiener et al., 1988).

Although all four methods applied to the simulation of Feller et al. give smaller values for V_L than the experimental values, the differences are still less than 1%. This supports the validity of the simulations. Moreover, the average of the 4c and 7c partitioning results is within experimental error of the average of the more accurate results obtained using Eq. 8 or Eq. 9. The partitioning methods require the assumption that the component volumes are constant as z is varied. These closely similar results for V_L offer modest support for that assumption.

The best support for the assumption that the component volumes are constant as a function of z is in the results for $p_T(z)$ shown in Figs. 2 and 3. Although the results in Fig. 2 for the 4c model show substantial deviations of $p_T(z)$ from 1 in the headgroup region, this can be understood as being due to the halo effect of large groups surrounded by smaller groups. As shown in Fig. 3, the halo effect disappears in model 7c when the headgroups are divided into substituents that are more comparable in size to the other groups. Although some systematic deviations remain in Fig. 3, these are at the 1% level, which appears to be the level of accuracy and validity of these methods and of the simulations.

We next turn to the results for the headgroup. Previous values for the volume V_H of the entire headgroup given by this laboratory include 344 Å^3 (Nagle and Wilkinson, 1978), 348 Å^3 (Nagle and Wiener, 1988), 340 Å^3 (Wiener et al., 1989), and 319 Å^3 (Sun et al., 1994). All of these values used gel phase or subgel phase data. Our most precise determination of gel phase structure (Sun et al., 1994) gives the smallest value of V_H. It has been argued (Nagle and Wilkinson, 1978; Wiener et al., 1988) that V_H is independent of the thermodynamic phase. The good agreement between the V_H obtained in Table 1 for a fluid phase simulation (324–326 Å^3) and our experimental V_H for the gel phase supports this assumption, and it supports our lower value of V_H, which is also near the value $V_H = 325$ Å^3 proposed by Small (1967).

The results for the 7c method shown in Table 1 give the molecular volumes for the components of the headgroup. Such detailed volumes have seldom been discussed in the literature. Wiener and White (1992) gave values for these volumes, but these depended upon less well founded results, including some of the older ones reported in the preceding paragraph. Their values were $V_{COO} = 36$ Å^3, $V_{gl} = 72$ Å^3, $V_{PO_4} = 70$ Å^3, and $V_{chol} = 134$ Å^3, with an overall $V_H = 348$ Å^3. The greatest difference between their values and our values in Table 1 is for V_{chol}; this is related to their use of the estimate of Small (1967) that $V_{chol} + V_{PO_4} = 204$ Å^3. (We note that use of a smaller value for V_{chol} would appear to improve the result of the test that Wiener and White apply to their data in their figure 7.)

We now turn to experimental results for the hydrocarbon chains. The experimental results for methylene volumes V_2 and methyl volumes V_3, summarized in Table 1, do not follow unambiguously from experimental data. There have been two notably different ways to obtain these volumes, as discussed in the appendix to the paper by Nagle and Wiener (1988). Both use data for saturated phosphatidylcholines (as well as alkanes) of varying chain lengths. The difference is whether the experimental data for the different chain lengths are compared at the same temperature or at the same reduced temperature. The first way, preferred by Nagle and Wilkinson (1978), yields a ratio $r = V_3/V_2 = 2.0$. The latter way, preferred by Small (1986), yields substantially different values, $V_2 = 29.6$ Å^3, $V_3 = 35.6$ Å^3 with a ratio $r = 1.20$. The present partitioning methods, 4c and 7c, for interpreting simulation results are quite independent of both previous ways of finding V_2 and V_3 from experimental volumetric data. The results presented in Table 1 strongly support the former way of interpreting the experimental data. In particular, the ratio r is 1.92 for the 7c method and 1.87 for the 4c method, reasonably close to the value $r = 2.0$ for the first interpretation of the experimental data and considerably larger than the value $r = 1.2$ from the second interpretation. A different simulation (Tu et al., 1995) yields $r = 2.0$, as shown in figure 8 of Nagle et al. (1996). This is an example in which simulation results are very helpful in deciding between conflicting interpretations of experimental data. It may also be noted that Wiener and White (1992) found a value of r close to 2.1 from their study of 1,2-dioleoyl-*sn*-glycero-3-phosphocholine at 67% relative humidity, where there were many more x-ray and neutron reflections for refining a packing model.

Guided by the present simulations (Feller et al., manuscript in preparation), we will take the value of r in this paper to be 1.9. Then, V_2 and V_3 can be determined by using $V_L - V_H = 28V_2 + 2V_3$ and $V_3 = rV_2$ (the ensuing volumes are shown in the Exp column of Table 1). This illustrates how the simulations, by supplying r, can be used to interpret the volumetric data. It may also be noted that the value of V_2 is larger than the previous value of 27.6 Å^3 (Nagle and Wiener, 1988). This change in V_2 is due to the more accurate wide-angle gel phase data of Sun et al. (1994) and is independent of the simulations, provided that a reasonable value of r is chosen. This semiempirical result for V_2, in turn, provides a test of whether the steric, excluded volume

effect is properly modeled in the simulation, inasmuch as one could have the correct ratio r, but with V_2 and V_3 scaled by the same incorrect constant factor. The good agreement of the values for V_2 and V_3 in either the 4c or the 7c columns in Table 1 with the values in the Exp column suggest that the simulations pass this test.

The concept of free volume is easily incorporated into our formalism, at least in an average fashion. A bare volume for each component is first defined, for example, from crystal studies. The free volume is then just the difference between the component volume and the bare volume. We have tested this procedure for consistency in the hydrocarbon region using the simulation results. The total free volume as a function of z was obtained by determining the fraction of the volume that may be occupied by zero-radius guest atoms without steric hindrance with the host molecules. This free volume was at maximum at about 29% in the center of the bilayer, and at 10 Å from the center it decreased to about 22%. We modeled this z dependence of the free volume, with deviations of $\pm 1\%$, by assigning bare volumes, $V_2^{\text{bare}} = 21.7$ Å^3 and $V_3^{\text{bare}} = 32.9$ Å^3. Notice that even though the component volumes and the bare volumes are not allowed to vary with z, the total free volume may. This is possible because the ratio of bare volumes, defined to be $r^{\text{bare}} = V_3^{\text{bare}}/V_2^{\text{bare}}$, is only 1.5, which is smaller than the ratio $r = 1.9$ of component volumes. Therefore, the terminal methyl free volume is relatively larger than the methylene free volume. Because the number density of terminal methyls is higher in the center of the bilayer, the total free volume is larger in the center, consistent with the conventional picture of lipid bilayers.

In conclusion, we have proposed a method for extracting volumes of substituent molecular groups in lipid bilayers that is both simple and computationally efficient, requiring only histograms of positions of the component groups that are customary to compute for other purposes. Although this method involves the fundamental assumption that each molecular group has constant component volume throughout the bilayer, there is an internal check on this assumption through the constancy of the total probability $p_T(z)$ as a function of z. Where firm experimental results are available, such as for V_L, the results of the method and the simulation appear to be reliable. This encourages use of this method to obtain results from simulations for those component volumes that are less firmly established experimentally.

We thank Drs. Stephanie Tristram-Nagle and Richard Pastor for helpful comments.

This research was supported by National Institutes of Health grant GM-44976-07.

REFERENCES

Blazyk, J. F., D. L. Melchior, and J. M. Steim. 1975. An automated differential scanning dilatometer. *Anal. Biochem.* 68:586–599.

Dufourc, E. J., C. Mayer, J. Stohrer, G. Althoff, and G. Kothe. 1992. Dynamics of phosphate head groups in biomembranes. *Biophys. J.* 61:42–57.

Laggner, P., K. Lohner, G. Degovics, K. Muller, and A. Schuster. 1987. Structure and thermodynamics of the DHPC-water system. *Mol. Cryst. Liq. Cryst.* 44:31–60.

Nagle, J. F. 1980. Theory of the main lipid bilayer phase transition. *Annu. Rev. Phys. Chem.* 31:157–195.

Nagle, J. F. 1993. Area/lipid of bilayers from NMR. *Biophys. J.* 64: 1476–1481.

Nagle, J. F., and M. C. Wiener. 1988. Structure of fully hydrated bilayer dispersions. *Biochim. Biophys. Acta.* 942:1–10.

Nagle, J. F., and M. C. Wiener. 1989. Relations for lipid bilayers: connection of electron density profiles to other structural quantities. *Biophys. J.* 64:1476–1481.

Nagle, J. F., and D. A. Wilkinson. 1978. Lecithin bilayers: density measurements and molecular interactions. *Biophys. J.* 23:159–175.

Nagle, J. F., R. Zhang, S. Tristram-Nagle, W.-J. Sun, H. I. Petrache, and R. M. Suter. 1996. X-ray structure determination of fully hydrated L_α phase dipalmitoylphosphatidylcholine bilayers. *Biophys. J.* 70:1419–1431.

Small, D. M. 1967. Phase equilibria and structure of dry and hydrated egg lecithin. *J. Lipid Res.* 8:551–557.

Small, D. M. 1986. The physical chemistry of lipids. *In* Handbook of Lipid Research, Vol. 4. Plenum Press, New York.

Sun, W.-J., R. M. Suter, M. A. Knewtson, C. R. Worthington, S. Tristram-Nagle, R. Zhang, and J. F. Nagle. 1994. Order and disorder in fully hydrated unoriented bilayers of gel phase DPPC. *Physiol. Rev.* 49: 4665–4676.

Tu, K., D. J. Tobias, and M. L. Klein. 1995. Constant pressure and temperature molecular dynamics simulation of a fully hydrated liquid crystal phase dipalmitoylphosphatidylcholine bilayer. *Biophys. J.* 69: 2558–2562.

Wiener, M. C., R. M. Suter, and J. F. Nagle. 1989. Structure of the fully hydrated gel phase of DPPC. *Biophys. J.* 55:315–325.

Wiener, M. C., S. Tristram-Nagle, D. A. Wilkinson, L. E. Campbell, and J. F. Nagle. 1988. Specific volumes of lipids in fully hydrated bilayer dispersions. *Biochim. Biophys. Acta.* 938:135–142.

Wiener, M. C., and S. H. White. 1992. Structure of fluid DOPC determined by joint refinement of x-ray and neutron diffraction data. III. Complete structure. *Biophys. J.* 61:434–447.